Enzymatic Hydrolysis Combined with Mechanical Shearing and High-Pressure Homogenization for Nanoscale Cellulose Fibrils and Strong Gels

M. Pääkkö,[†,‡] M. Ankerfors,[§] H. Kosonen,[†] A. Nykänen,[†] S. Ahola,[∥] M. Österberg,[∥] J. Ruokolainen,[†] J. Laine,[∥] P. T. Larsson,[§] O. Ikkala,*[,†] and T. Lindström*[,§]

Laboratory of Optics and Molecular Materials, Department of Engineering Physics and Mathematics and Center for New Materials, Helsinki University of Technology, P.O. Box 2200, FIN-02015 HUT, Espoo, Finland, STFI-Packforsk AB, P.O. Box 5604, SE-114 86 Stockholm, Sweden, Department of Fibre and Polymer Technology, Royal Institute of Technology, KTH, Stockholm, Sweden, Molecular Electronics and Nanotechnology, Physics Department, SNIAM Building, Trinity College, Dublin, Ireland, and Laboratory of Forest Products Chemistry, Department of Forest Products Technology, Helsinki University of Technology P.O. Box 6300, FIN-02015 HUT, Espoo, Finland

Received December 22, 2006; Revised Manuscript Received March 9, 2007

Toward exploiting the attractive mechanical properties of cellulose I nanoelements, a novel route is demonstrated, which combines enzymatic hydrolysis and mechanical shearing. Previously, an aggressive acid hydrolysis and sonication of cellulose I containing fibers was shown to lead to a network of weakly hydrogen-bonded rodlike cellulose elements typically with a low aspect ratio. On the other hand, high mechanical shearing resulted in longer and entangled nanoscale cellulose elements leading to stronger networks and gels. Nevertheless, a widespread use of the latter concept has been hindered because of lack of feasible methods of preparation, suggesting a combination of mild hydrolysis and shearing to disintegrate cellulose I containing fibers into high aspect ratio cellulose I nanoscale elements. In this work, mild enzymatic hydrolysis has been introduced and combined with mechanical shearing and a high-pressure homogenization, leading to a controlled fibrillation down to nanoscale and a network of long and highly entangled cellulose I elements. The resulting strong aqueous gels exhibit more than 5 orders of magnitude tunable storage modulus G' upon changing the concentration. Cryotransmission electron microscopy, atomic force microscopy, and cross-polarization/magic-angle spinning (CP/MAS) ^{13}C NMR suggest that the cellulose I structural elements obtained are dominated by two fractions, one with lateral dimension of 5−6 nm and one with lateral dimensions of about 10−20 nm. The thicker diameter regions may act as the junction zones for the networks. The resulting material will herein be referred to as MFC (microfibrillated cellulose). Dynamical rheology showed that the aqueous suspensions behaved as gels in the whole investigated concentration range 0.125−5.9% w/w, G' ranging from 1.5 Pa to 10^5 Pa. The maximum G' was high, about 2 orders of magnitude larger than typically observed for the corresponding nonentangled low aspect ratio cellulose I gels, and G' scales with concentration with the power of approximately three. The described preparation method of MFC allows control over the final properties that opens novel applications in materials science, for example, as reinforcement in composites and as templates for surface modification.

Introduction

There exists a growing interest in cellulose I beyond its extensively studied classic applications as its abundance, biological origin, and inherent properties encourage the utilization of nanoscale cellulose I elements for a variety of potential novel applications. Cellulose I is made from glucan, a linear, high-molecular weight natural polymer consisting of repeating β-(1→4)-D-glucopyranose units.[1] The revived interest is because the cellulose present in macroscopic fibers obtained from, for example, plants consists of a hierarchical structure built up by smaller and mechanically stronger entities. The smallest discernible building block of cellulose I is a bundle of parallel glucan chains, typically with a square or close-to-square cross section, herein referred to as a cellulose I fibril. Such fibrils aggregate as fibril aggregates. For typical wood pulp fibers, the lateral dimension of fibrils is about 5 nm and for fibril aggregates about 20 nm, depending both on species and history.[2,3] The strong mutual packing of fibrils in a fibril aggregate makes them difficult to disintegrate. Fibril aggregates are characteristic for cellulose I from plant fibers. The finite lateral dimension of the fibrils prevents that all glucan chains would be crystallized, as the glucan chains belonging to the surface of the fibrils are considered noncrystalline. Localized distortions along the transverse direction of the fibril can also contribute to the amount of noncrystalline glucan chains and form "weak spots" with an increased susceptibility for, for example, hydrolysis. Mercerization or regeneration changes the crystalline cellulose I structure partially or completely to cellulose II, which is a form of cellulose with antiparallel glucan chains.[4,5]

Several routes to prepare fibrils or fibril aggregates have been described: A straightforward concept is based on dissolution

* To whom correspondence should be addressed. E-mail: tom.lindstrom@stfi.se (T. L.), Olli.Ikkala@hut.fi (O. I.).
† Optics and Molecular Materials.
‡ Molecular Electronics and Nanotechnology.
§ STFI-Packforsk AB.
∥ Laboratory of Forest Products.

10.1021/bm061215p CCC: $37.00 © 2007 American Chemical Society
Published on Web 05/03/2007

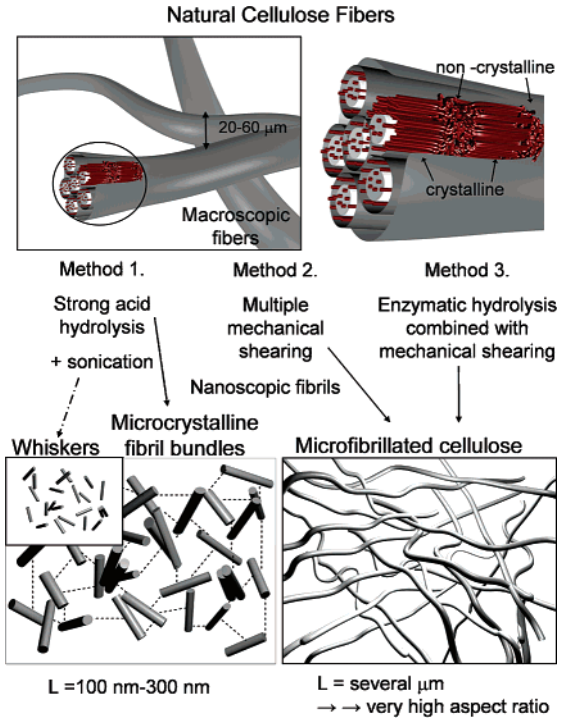

Figure 1. Two methods to disintegrate macroscopic cellulosic fibers into nanoscale fibrils. For simplicity, the constituent fibrils are not drawn rectangular. In method 1, aggressive acid hydrolysis leads to colloidal suspension of aggregated, highly crystalline, and low aspect ratio fibril aggregates.[8,9,22−25] Further hydrolysis and sonication breaks down fibril aggregates to cellulose fibrils, i.e., whiskers, which form a weak physical network (- - -) by hydrogen bonds.[10−12] Microfibrillated cellulose (MFC) is classically prepared by disintegration by application of high shear forces (method 2) which leads to highly entangled and inherently connected fibrils and fibril aggregates and mechanically strong networks.[15−17] The present work (method 3) incorporates an additional enzymatic hydrolysis[29] which yields a mixture of dominantly cellulose I fibrils (about 5 nm thickness) and fibril aggregates (about 10−20 nm thickness).

in solvents, regeneration, and even potentially electrospinning[6,7] where the dissolution process leads to structural elements of the cellulose II[4,5] type, which typically has reduced strength. If a complete dissolution is not preferred and, instead, disintegration down to the level of the mechanically strong cellulose I fibrils or fibril aggregates is pursued, two main concepts have been described: Strongly acidic conditions combined with sonication lead to aggressive hydrolysis to attack the noncrystalline fractions. This results in mainly low aspect ratio cellulose I fibril aggregates and fibrils which are also denoted as whiskers,[8−12] see Figure 1. The relatively low aspect ratio and rodlike character is useful to prepare chiral nematic phases in aqueous media[10,11,13] but leads to mechanically relatively weak gels, which are not particularly suitable for mechanical reinforcement.

For pursuing applications which require extensively entangled networks and higher strength, chemically less aggressive hydrolysis[14] concepts have been found to maintain a high aspect ratio of the cellulose I fibrils or fibril aggregates, potentially allowing strong or even permanent junction points for the networks. A classic example is provided by omitting the hydrolysis step altogether and by solely imposing high shearing forces for disintegration. This yields a highly entangled network which typically consists of elements having a wide size distribution down to nanoscale.[15−17] The resulting material has been denoted microfibrillated cellulose (MFC), originally introduced by Turbak et al.[15] and Herrick et al.[16] The degree of crystallinity is usually low, as a substantial part of the noncrystalline domains remains essentially intact, resulting in a high aspect ratio. Such an MFC forms strongly entangled and disordered networks and gels because of entanglements and junction zones probably because of partially disintegrated fibril aggregates (Figure 1). It is important that in this case the networks are inherent, and gels can become much stronger than in the case when the network is formed only because of weak hydrogen bonds between water and fibrils, as in low aspect ratio cellulose I fibrils or fibril aggregates obtained by acid hydrolysis. Therefore, MFC and other inherent cellulose networks also allow efficient reinforcement of nanocomposites at low concentrations.[18−20]

The preparation of MFC solely by shear forces is accompanied with a serious problem. To prepare MFC in a well-controlled manner by this strategy, the shearing energy required is excessive, therefore requiring multiple passes[17] through the homogenizer, and additionally the process is prohibitively unstable as the constrictions of homogenizers tend to quickly be blocked.

In this work, it is demonstrated that a combination of high-pressure shear forces and mild enzymatic hydrolysis[21] constitutes a new and efficient method to prepare MFC with a well-controlled diameter in the nanometer range and to maintain high aspect ratio, in contrast to acid hydrolysis. In particular, it is demonstrated that strong aqueous gels with highly tunable storage modulus can be obtained which suggests application of MFC to reinforce multicomponent mixtures. The aqueous gel structure has been investigated by cryo-transmission electron microscopy (TEM) in bulk and by atomic force microscopy (AFM) from dried samples on substrates. Comprehensive dynamic rheology has been investigated and compared with rheology of nonentangled rodlike cellulose "nanocrystallites" or "nanofibrillar" networks from the dissolved and precipitated cellulose II gels.[11,12,22−28]

Finally, in the previous literature, there seems to be lack of generally accepted definitions: MFC has been used to denote qualitatively different compounds and typical MFC made from wood fibers may contain considerable amounts of hemicelluloses, leading to widely different properties.

Experimental Section

Materials. The bleached sulfite softwood cellulose pulp (Domsjö ECO Bright; Domsjö Fabriker AB) consisting 40% pine (*Pinus sylvestris*) and 60% spruce (*Picea abies*) with a hemicellulose content of 13.8% (measured as solubility in 18% NaOH, R18[30]) and a lignin content of 1% (estimated to 0.165*Kappa number (SCAN C 1:00)) was used as a source for the microfibrillated cellulose. The pulp was used in its never-dried form. The phosphate buffer used during the enzymatic treatment was prepared from 11 mM KH_2PO_4 and 9 mM Na_2HPO_4 so that pH was between 6.8 and 7.2, and the enzyme used was a monocomponent endoglucanase (Novozym 476, Novozym A/S) which was used without further purification. The microbicide used after the pretreatment was 5-chloro-2-ethyl-4-isothiazolin-3-one (Nalco AB, Sweden).

Gel Preparation. The cell wall delamination was carried out by treating the sulfite pulp in four steps: first, a refining step to increase the accessibility of the cell wall to the subsequent monocomponent endoglucanase treatment, an enzymatic treatment step, a second refining stage, and finally the pulp slurry was passed through a high-pressure homogenizer (Scheme 1). Hence, a 4% w/w cellulose suspension was mechanically refined using an Escher-Wyss refiner (Angle Refiner R1L, Escher-Wyss) with 33 kWh/tonne at a specific edge load of 2 Ws/m to 28 °SR (see ref 31). Next, the enzyme was added. In this enzymatic treatment, 100 g (calculated as dry fibers) of the refined pulp was

Scheme 1. A Method for Producing Microfibrillated Cellulose Gel by Combined Refining, Enzymatic Treatment, and High-Pressure Homogenization

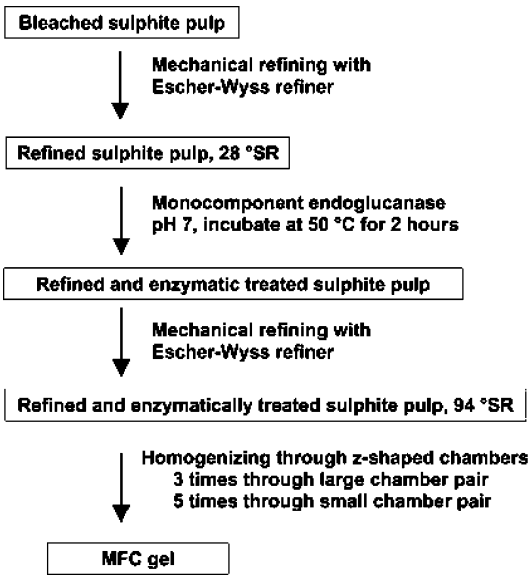

dispersed in 2.5 L of phosphate buffer (pH 7, final pulp concentration 4% w/w) with 0.17 μL monocomponent endoglucanases per gram fiber (5 ECU/μL) and was incubated at 50 °C for 2 h. The samples were mixed manually every 30 min. Then, the samples were washed with deionized water and the monocomponent endoglucanase was denaturated at 80 °C for 30 min. At the end, the pulp sample was washed with deionized water again. The prerefined and enzyme-treated pulp was refined once again with the Escher-Wyss refiner, this time, to 94 °SR (average refining energy 90 kWh/tonne, specific edge load 1 Ws/m). To prevent a bacterial growth in the material, 0.4 μL/mL of microbicide, 5-chloro-2-methyl-4-isothiazolin-3-one, was added to the slurry. Subsequently, the material was passed through a high-pressure fluidizer (Microfluidizer M-110EH, Microfluidics Corp.). The pulp fiber slurry of 2% w/w concentration was passed through two differently sized Z-shaped chamber pairs (each pair connected in series). First, the slurry passed three times through a chamber pair with a diameter of 400 μm and 200 μm (the first chamber and the second chamber, respectively), and then five times through a chamber pair with a diameter of 200 μm and 100 μm. The operating pressures were 105 and 170 MPa, respectively. The 3% w/w and 5.9% w/w samples and the 0.125−1.5% w/w samples were prepared from the standard 2% w/w MFC gel by filtration and diluting the MFC, respectively. After the filtration and dilution, the samples were dispersed with a high intensity mixer (Polytron PT 3000, Kinematica AG) at 4000 RPM for 15 s.

Transmission Electron Microscopy. A thin film of MFC gel was frozen from room temperature and 100% humidity with a Tecnai Vitrobot. A 2% MFC gel was applied on glow discharge treated Quantifoil holey carbon copper grid with the hole size of 2 μm. The grid was blotted multiple times and then was shot to liquid ethane of temperature −175 °C. The grid with vitrified gel film was cryotransferred into a Tecnai 12 transmission electron microscope with Gatan 910 cryotransfer holder, which was cooled below −180 °C. Bright-field TEM was performed using an acceleration voltage of 120 kV.

Atomic Force Microscopy. The properties of MFC were also determined using a Nanoscope IIIa Multimode scanning probe microscope (Digital Instruments Inc., Santa Barbara, CA). A drop of very dilute MFC suspension (0.05% w/w) was allowed to dry at room temperature overnight on a clean mica substrate. The images were scanned in tapping mode in air using silicon cantilevers (NSC15/AIBS) delivered by MicroMash (Tallinn, Estonia). The drive frequency of the cantilever was about 305−325 kHz. The size of the images was 1 × 1 μm and 5 × 5 μm, and the images were scanned across 10 different parts of the sample. No image processing except flattening was made.

NMR Spectroscopy and Spectral Fitting. The MFC sample was ultracentrifuged (150 000*g*, 30 min) to a solids content of approximately 15−20% w/w. Cross-polarization/magic-angle spinning (CP/MAS) ^{13}C NMR spectrum (64k transients) was then recorded (at 292 ± 1 K) using a Bruker AQS-300 instrument operating at 7.05 T. A double air-bearing probe and a zirconium oxide rotor were employed. The MAS rate was 5 kHz. A CP pulse sequence was based on a 4.0 μs proton 90° pulse, 800 μs ramped (100−50%) contact pulse, and a 2.5 s delay between repetitions. A TPPM15 pulse sequence was used for 1H decoupling. Glycine was used for the Hartmann−Hahn matching procedure as well as an external standard for calibration of the chemical shift scale relative to tetramethylsilane ($(CH_3)_4Si$). The glycine carbonyl line was assigned a chemical shift of 176.03 ppm.

Lateral fibril dimensions (LFD) and lateral fibril aggregate dimensions (LFAD) can be determined from CP/MAS ^{13}C NMR spectra recorded on cellulose I samples. For this purpose, the C4-region of the spectrum is subjected to spectral fitting as described in detail elsewhere.[32,33] The development and implementation of the software was made at STFI-Packforsk and is based on the Levenberg−Marquardt method.[34]

For isolated cellulose I, discernible and quantitative signals exist for the C4 atoms of the glucan chains located in the interior parts of the fibrils and for C4 atoms in glucan chains located at fibril surfaces. Using the integrated signal intensity for the entire C4 region of the spectra and the integrated intensity for the C4 surface signals (both obtained from the spectral fitting procedure), LFD and LFAD can be estimated under the assumption of a square cross section of both fibrils and fibril aggregates. Therefore, the measured LFD and LFAD are expressed as a ratio of the number of glucan chains present at surfaces divided by the total number of glucan chains in either the fibril or fibril aggregate. This can be converted to dimension by using a fixed conversion factor of the individual width of a glucan chain, that is, 0.57 nm.

In the fitting of CP/MAS ^{13}C NMR spectra, the hemicellulose gives signals that interfere with the signals from cellulose. This can result in diverging rather than a converging fitting procedure. To obtain estimates for LFD and LFAD without a need to chemically remove the hemicellulose, one of the 24 parameters adjusted during the fitting procedure was held constant, the signal position of the signal originating from C4 atoms in glucan chains at inaccessible fibril surfaces (84.2 ppm).

Dynamic Rheology. Dynamic rheology was measured using a controlled strain rheometer (AR 2000, TA Instruments) using two different geometries: cone-and-plate (cone angle 1°) and plate-and-plate. An acrylic 60 mm plate was used for the 0.125−0.5% samples, an aluminum 40 mm cone was used for the 1−3% w/w samples, and a 20 mm steel plate was used for the 5.9% w/w sample. The different geometries were used to obtain the best sensitivity for the different viscosity levels. The gap was 1 mm for the plate-and-plate geometry. Before each measurement, the samples were allowed to rest for 5−10 min. Covers around samples and silicon oil were used to avoid the sample drying at higher temperatures. Before the dynamic viscoelastic measurements, the linear viscoelastic region was determined by torque sweeps for all suspensions. The torque sweeps were measured for 0.01−100 Pa at the frequency of 1 Hz. The chosen dynamic strain amplitudes for the frequency sweep measurements were 0.06 for the 5.9% w/w suspensions and 0.25 (0.2) for the 2−0.125% w/w suspensions at which they showed linear viscoelasticity. The frequency sweeps were carried out in the range of 0.01−100 Hz at the linear viscoelastic region, controlling the strain. The effect of temperature on gel properties was studied for 20−80 °C at 1 Hz using the linear viscoelastic region. Shear viscosity was monitored by increasing the shear rate from 0.1 to 1000 1/s at 25 °C.

Charge Measurement. Prior to the charge measurement, the MFC was set to its hydrogen counterion form as follows. A sample containing 4.5 g of dry MFC was dispersed in 600 mL of deionized water. The dispersion was centrifuged at 3600*g* for 15 min. The clear phase was

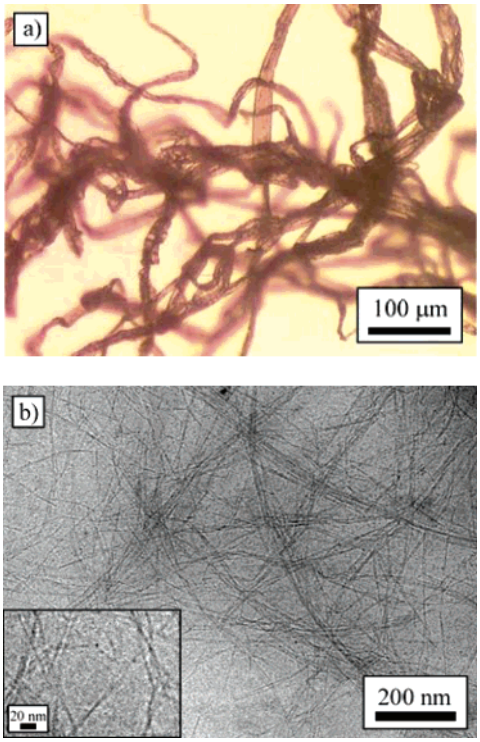

Figure 2. (a) Optical micrograph of original sulfite cellulose macroscopic fibers of sizes of several tens of μm. (b) Cryo-TEM of the frozen 2% w/w MFC gel after the refining, enzymatic hydrolysis, and homogenization processes, showing a fibrillated network of nanoscale fibrils, mostly with a diameter of ca. 5−6 nm and occasionally thicker fibril bundles potentially forming the junction zones.

removed and filtrated (Munktell Filter Paper quality "3"), and the collected dry sample was recovered. To set the MFC to its hydrogen counterion form, the MFC was dispersed in deionized water and 0.01 M HCl was added, fixing pH to 2. The excessive HCl was washed away after 30 min by dispersing the sample to deionized water and centrifuging it as above. The washing procedure was performed several times until the conductivity was <5 μS/cm.

To set the MFC to its sodium counterion form, it was dispersed in deionized water and then 0.001 M $NaHCO_3$ was added. After 10 min, pH was set to 10 using NaOH. After 30 more minutes, the excess NaOH and the $NaHCO_3$ were washed away by dispersing the sample with deionized water and centrifuging it several times until the conductivity was <5 μS/cm. After this, the sample was once more set to its hydrogen counterion form and washed the conductivity to be again <5 μS/cm. Finally, the total charge density of the MFC was measured with conductometric titration according to the procedure described elsewhere.[35]

Results and Discussion

To facilitate the disintegration of the constituent fibrils into nanoscale fibrils, sulfite pulp with high hemicellulose content was selected. The original sulfite cellulose pulp fibers are tens of micrometers in diameter and are best visualized in optical microscopy, see Figure 2a. As a reference, and to demonstrate the importance of the enzymatic hydrolysis step, an attempt was made to prepare MFC only by extensive mechanical shearing using the homogenizer. The constriction chambers of the homogenizer quickly became blocked and the resulting material was nonhomogeneous and contained a large fraction of intact fibers. These observations, in combination with the high required energy, indicated that a sole mechanical shearing is not a feasible preparation method and does not yield well-defined nanoscale

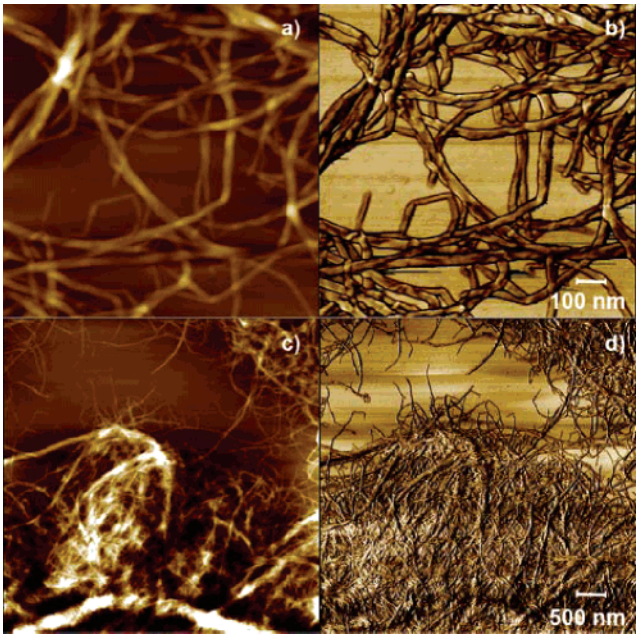

Figure 3. AFM images of microfibrillated cellulose on mica after drying: topographical images (a and c), and phase-contrast images (b and d). The scan size was 1×1 μm (a and b) and 5×5 μm (c and d). The images illustrate dried fibrils of height of ca. 5 nm and width of ca. 20−30 nm. The sample has been prepared using the 2% w/w aqueous suspension which has been diluted to the concentration of ca. 0.05% w/w.

cellulose I elements. Since typical strong acid hydrolysis is aggressive, yielding low aspect ratio cellulose I elements, a less aggressive enzymatic hydrolysis was used. It turned out that the use of a monocomponent endoglucanase allowed a selective hydrolysis[29] of the noncrystalline cellulose allowing mechanical disintegration of fibers into high aspect ratio nanoscale cellulose I elements. The high hemicellulose content of the present pulp decreases the cell wall cohesion of the fibers, making cell wall delamination easier. This is, however, not sufficient to avoid blocking of the constriction chambers of the homogenizer and to decrease the required energy consumption. It was found that small additions of the monocomponent endoglucanase enzyme promoted cell wall delamination and prevented the blocking of the homogenizer. It is important to avoid hydrolysis of the hemicellulose, and therefore a pure endoglucanase was selected. The sulfite fibers were first mechanically refined to introduce damage zones in the cellulose I and to swell the fiber wall. This is believed to enhance the effect of the enzyme treatment by creating a controllable amount of weak points within the fiber cell wall that facilitates the mechanical disintegration. The resulting material is a slightly opaque gel-like aqueous matter, having an MFC concentration of 2% w/w. Different concentrations were explored and the 2% w/w concentration was found to be most suitable for the stability of the process. Other concentrations were prepared from this stock suspension by either dilution or concentration. In addition, there exists an optimum enzymatic dose. No enzymatic treatment leads to blocking and a too high dosage (30 μL monocomponent endoglucanases per gram fiber (5 ECU/μL)) decreases the refining and homogenization efficiency.

The morphology of the resulting nanoscale fibrils after the mechanical, enzymatic, and high-pressure homogenization steps is shown in Figure 2b for a frozen gel (cryo-TEM) and for dried microfibrils on mica substrates in Figure 3 (AFM). Interestingly, cryo-TEM shows long, well-defined, and distinct cellulose microfibrils which are mostly of diameter of ca. 5 nm as well

CDV

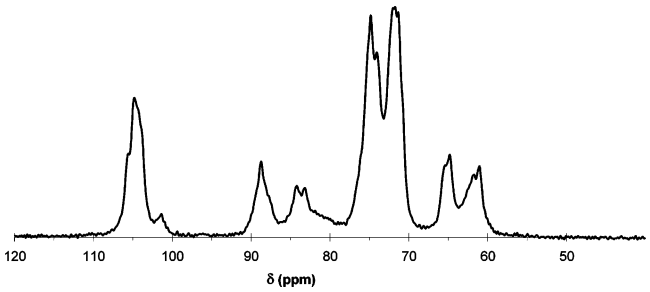

Figure 4. The CP/MAS ^{13}C-NMR spectra for MFC 2% w/w sample. The C4 spectral region (about 78−92 ppm) is used for spectral fitting and subsequent determination of cellulose I fibril and fibril aggregate widths (LFD and LFAD).

as thicker fibrils of diameter of up to 10−20 nm. Particular efforts have been paid to suppress drying during the cryo-TEM procedure, which therefore may promote the observation of comprehensive fraction of well-defined single fibrils.

The AFM micrograph of a dried sample on mica substrate shows a network of objects whose width is 20−30 nm but the height is less, ca. 5 nm. The larger width of the fibrils as compared to those in the cryo-TEM-images can be due to the drying of fibrils or fibril aggregates which affects the dimensions because aggregation or flattening may occur. In addition, the actual size of the AFM tip introduces a small error in the measured diameters of the fibrils. A fraction of thicker fibril aggregate bundles can also be observed from the AFM images. Importantly, it is concluded that the obtained cellulose fibrils are interconnected and coiled and form an inherently entangled network, in contrast to nonentangled acid hydrolyzed and sonicated rodlike cellulose crystallites[10−13,36,37] or less entangled microfibrils.[9,22−26,28]

CP/MAS ^{13}C-NMR spectra were useful to characterize the 2% w/w MFC sample, see Figure 4. Spectral fitting suggests that the lateral fibril dimensions (LFD) and the lateral fibril aggregate dimensions (LFAD) are 4.6 nm (standard error = 0.1) and 17.3 nm (standard error = 0.7), respectively, in good agreement with the results obtained from both TEM and AFM measurements. The presence of residual hemicelluloses interfered with the determination of LFD and LFAD from the spectra, and therefore the results remain semiquantitative. In addition, a semiquantitative estimate for the fraction of the glucane chains in crystalline parts can be estimated, leading to an estimated crystallinity of ca. 8−12%, that is, relatively low. Finally, an effort was made to assess the crystalline allomorph composition. For the MFC samples, both the low solid content (resulting in low signal-to-noise ratios in the recorded spectra) and the smallness of the LFD made such estimates difficult. The only discernible signal from the glucan chains in the crystalline cellulose moieties was the cellulose $I(\alpha + \beta)$ signal (88.8 ppm), shown in Figure 4. Therefore, no definite statement can be made regarding the dominating cellulose I allomorph in the MFC.

An entangled network structure should manifest itself in mechanical and viscoelastic properties and in gelation. The rheological properties of the aqueous suspensions are discussed next, see Figure 5. The lower MFC concentrations were obtained from the 2% w/w suspension by dilution, followed by high intensity mixing, and the higher concentrations were obtained by evaporation of water. It was found that G' and G'' were relatively independent of the angular frequency at all of the investigated concentrations. In classical viscous fluids, the elastic and loss modulus have a characteristic frequency dependency, that is, $G' \propto \omega^2$ and $G'' \propto \omega^1$ where $G' \ll G''$, whereas an

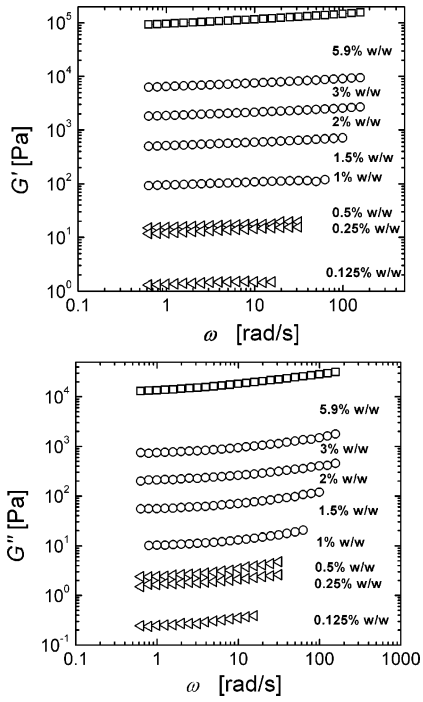

Figure 5. The storage modulus (G') and the loss modulus (G'') as a function of frequency for all MFC suspensions. Geometries used: steel plate for 5.9% w/w, aluminum cone-and-plate for 1−3% w/w, and acrylic plate for 0.125−0.5% w/w.

ideal gel behaves elastically and $G' \propto \omega^0$, that is, the storage modulus is independent of the frequency, and $G' \gg G''$.[38] On the basis of Figure 5, a gel-like behavior was observed for all of the investigated MFC suspensions, even for the lowest concentration. Importantly, the values of the storage modulus are particularly high in comparison to the previously published results for nanoscale cellulose crystallites.[22−25] For example, 3% w/w of the present MFC leads to $G' \approx 10^4$ Pa, whereas 3% w/w of rodlike cellulose crystallites leads to $G' \approx 10^2$ Pa,[23] that is, a 2 orders of magnitude higher storage modulus. Similarly, a concentration of 2% w/w of MFC leads to $G' \approx 10^3$ Pa, whereas 2% w/w of modified rodlike cellulose crystallites leads to $G' \approx 10^1$ Pa.[25] The present higher elastic modulus is due to long fibrils and fibril aggregates forming an inherently entangled network structure in comparison to the more weakly interconnected low aspect ratio cellulose I elements. Another observation in the present case is that the elastic moduli are almost 10-fold in comparison to the loss moduli at the same concentration, also indicating a rather strong networking, even for the lowest concentration.

Furthermore, the loss tangent (tan δ) values, which measure the ratio of the loss modulus to the elastic modulus (G''/G'), were below 0.3 for all MFC suspensions: tan δ was ∼0.17 for 5.9−1% w/w suspensions, increasing to ∼0.24 for the range 0.5 −0.125% w/w. This is a further indication that all suspensions are predominantly elastic. It is interesting that the tan δ values for all suspensions were fairly equal. However, the tan δ of MFC at the lowest concentration exhibited the highest value, meaning that at low concentration there is a more viscous behavior than at high concentrations. All suspensions showed slightly reduced tan δ as a function of increasing frequency, meaning increased elasticity, that is, stronger gel.

The elastic modulus as a function of MFC concentration (Figure 6) shows a particularly strong concentration dependence, as the storage modulus increases 5 orders of magnitude upon increasing the concentration from 0.125% w/w to 5.9% w/w.

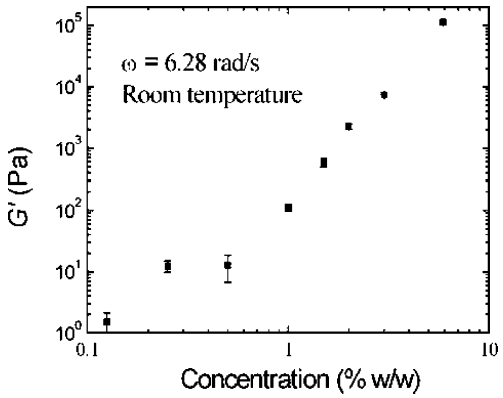

Figure 6. The storage modulus as a function of concentration at 25 °C and at the frequency of 1 Hz ($\omega = 6.28$ rad/s).

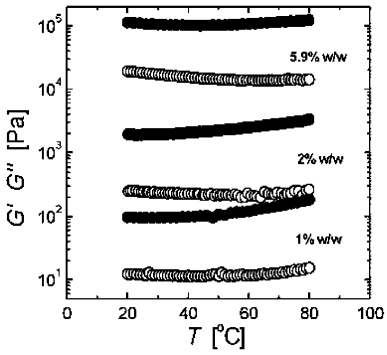

Figure 7. Storage and loss moduli as a function of temperature at 1 Hz for three different concentrations. G', closed symbols and G'', open symbols.

There exists considerable literature on the dependence of the modulus on the solvent concentration for various polymers and solvents (for a comprehensive discussion, see, e.g., refs 38 and 39). In many cases, a scaling relation $G \propto \phi^n$ has been observed, where ϕ = polymer concentration and $n \cong 1.8...2.0$, while in some cases much larger values $n \cong 4...7$ have been observed, for example, for polysaccharides in aqueous medium.[39] An early effort to explain the behavior was based on a scalar percolation model where a scaling $n \cong 2$ was predicted.[40] Later it was pointed out, in fact, that vector percolation models would be more appropriate.[41] Dissolution of rodlike tunicate (*Halocynthia roretzi*) cellulose nanocrystals, microcrystalline cellulose (MCC), or dissolving pulp in organic solvents leads to $n \cong 2.14$[42] which is quite near 2.25 as suggested by scaling theory[40] and Doi−Edwards theory.[43] In the present case, dealing with gelation of the highly entangled and rigid MFC, the model by Jones and Marques could be applicable.[39,44] Accordingly, with rigid networks with constrained, that is, frozen, junction zones, the elastic modulus is predicted to be $G \propto \phi^{(3+D_F)/(3-D_F)}$, where D_F is the fractal dimension of the objects connecting the junctions. With rodlike connectivity between the junction zones ($D_F = 1.0$), the scaling $G \propto \phi^2$ is predicted, thus explaining a wealth of experimental observations using different polymers including aqueous agarose and carrageenan.[38,39] Now, turning to Figure 6, the first conclusion is that the rise is much steeper than the classic observation $n = 2$. In fact, a straight line may not easily be fitted in the whole concentration range and even a kink near 0.5% w/w cannot be excluded. Still, definitely a steep rise is suggested, that is, $n \cong 3$. This value would suggest a fractal dimension $D_F \cong 1.5$.[45] It must, however, be emphasized that this consideration remains preliminary.

The temperature dependence of G' and G'' was also investigated, see Figure 7. The temperature sweeps from 20 °C to 80 °C were measured for the 5.9, 2, and 1% w/w suspensions using a frequency of 1 Hz, and they showed no dependence on temperature until 40 °C. The moduli increased very slightly with further increase of temperature from 50 °C to 80 °C, meaning that a slightly stronger network is formed at higher temperatures. This was also indicated by the tan δ values, which decreased with increasing temperature.

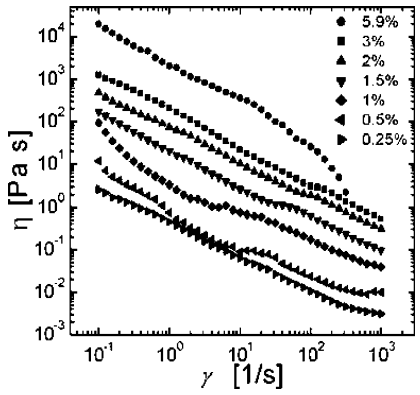

Figure 8. Influence of shear rate on the viscosity of different MFC concentrations (% w/w).

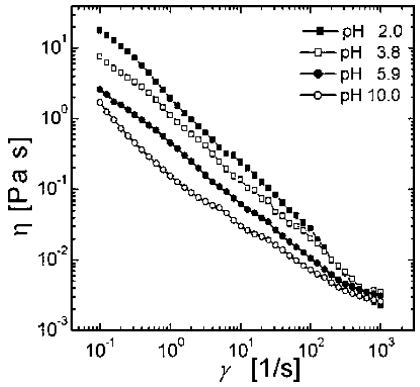

Figure 9. Influence of pH on viscosity of 0.25% w/w MFC.

In addition, the shear viscosities for different concentrations were investigated as a function of shear rate, see Figure 8. All suspensions show a large decrease of viscosity with increasing shear rate, that is, shear thinning. The shear thinning of MFC was already early recognized in the literature for the materials prepared solely by mechanical disintegration.[16] Therefore, an MFC gel can be considered as a pseudoplastic material. This behavior is also a characteristic of liquid crystals[46] and cellulose whiskers[11−13,36,37] or microcrystalline cellulose hydrogels.[24,27] However, the shear viscosity, for example, at the shear rate of 10 1/s, shows the evident structural difference between MFC and low aspect ratio cellulose I elements. Not surprisingly, the viscosity of the nonentangled 1% w/w cellulose I elements at shear rate of 10 1/s is $\sim 10^{-3}$ Pa s,[11,12] whereas in this case, the viscosity of 1% w/w MFC is $\sim 10^{-1}$ Pa s, that is, 2 orders of magnitude larger. In the case of the weakly bonded networks of low aspect ratio cellulose I elements, upon exposing increased shear rate, the network falls apart easily and individual elements start to flow. In the case of the more entangled networks of MFC, the viscosity remains higher.

The total charge of the original pulp and the MFC were the same before and after the treatments, that is, 44.2 μeq/g. Since practically all charges are due to the presence of hemicellulose, the hemicellulose content remained constant, as expected, during the MFC preparation process. These charges reduce the interfibrillar interactions because of electrostatic repulsion, and this is expected to lead to a lower viscosity. In Figure 9, the

dependence of pH on MFC shear thinning behavior is seen. At lower pH, the hydrogen ions neutralize the charges of the hemicellulose associated with the MFC which reduces the electrostatic repulsion, resulting in a higher interfibrillar interaction and a higher viscosity. At higher pH, on the other hand, the number of charges increases leading to a higher electrostatic repulsion resulting in a lower interaction and a lower viscosity.

Conclusions

A facile concept to prepare nanoscale cellulose fibrils is presented, where enzymatic hydrolysis is used in combination with mechanical shearing and high-pressure homogenization to promote delamination of the fiber wall. The milder hydrolysis as provided by enzymes in comparison to more aggressive acid hydrolysis allows longer and highly entangled nanoscale fibrils, whose feasibility in reinforcing multicomponent mixtures is here manifested by the observed strength of the gel networks down to low concentrations. On the basis of cryo-TEM and AFM and supported by CP/MAS ^{13}C-NMR, the resulting MFC appears to mainly consist of fibrils with a diameter of ca. 5−6 nm and fibril aggregates around 10−20 nm. Particularly strong aqueous gels are obtained, for example, $G' = 10^5$ Pa and 10^2 Pa at concentrations 5.9% w/w and 1% w/w using dynamic rheology at 1 Hz. The modulus of the gel can be tuned to values covering a wide range, that is, 5 orders of magnitude upon adjusting the concentration between 0.125 and 5.9% w/w, with an extensive shear thinning behavior. The incorporation of the enzymatic hydrolysis has a drastic effect, that is, using solely the mechanical shearing without enzymatic hydrolysis, sufficiently homogeneous materials could not be prepared because of severe blocking problems during the homogenization step. In contrast to the more aggressive acid hydrolysis, the milder enzymatic hydrolysis allows a higher aspect ratio of the resulting cellulose I elements and may partially preserve junction sites of the network. This leads to a drastically enhanced strength of the gel network. The well-controlled networking is reflected in the high elastic modulus, that is, roughly 2 orders of magnitude larger than for corresponding gels made by, for example, acid hydrolysis, and a G' scaling with concentration as the power of ca. 3. Finally, the enzymatic step leads to reduced energy consumption, thus allowing widespread use of the materials. The present nanoscale cellulose fibrils open several challenging options for materials science not only to tune the aqueous properties but also for totally new applications, such as templates for functional nanostructures.

Acknowledgment. The work has been performed as a part of "Nanostructured cellulose products" project in the Finnish-Swedish Wood Material Science Research Program in conjunction with the EU sixth framework IP "SustainPack" project. We acknowledge Prof. Lars Berglund and Prof. Lars Wågberg (KTH) for valuable discussions. Prof. Heikki Tenhu, Dr. Sami Hietala (Helsinki University, Laboratory of Polymer Chemistry), and Åsa Blademo (STFI-Packforsk AB) are acknowledged for valuable experimental assistance and numerous discussions. We acknowledge also Riitta Silvennoinen (TKK). The financial support from TEKES, VINNOVA, and numerous companies participating in the project is gratefully acknowledged. The funding from Ahlström Foundation, Research Foundation of Helsinki University of Technology, and the member companies of the STFI-Packforsk Paper Chemistry Cluster is gratefully acknowledged. This work was partly carried out in the Centre of Excellence of Finnish Academy ("Bio-and Nanopolymers Researcher Group", 77317).

References and Notes

(1) Meshitsuka, G.; Isogai, A. Chemical Structures of Cellulose Hemicellulose and Lignin. In *Chemical Modification of Lignocellulosic Materials*; Hon, D. N.-S., Ed.; Marcel Decker, Inc.: New York, 1996; pp 11−33.
(2) Hult, E. L.; Larsson, P. T.; Iversen, T. *Polymer* **2001**, *42*, 3309−3314.
(3) Hult, E. L.; Larsson, P. T.; Iversen, T. *Holzforschung* **2002**, *56*, 179−184.
(4) Atalla, R. H.; Vanderhart, D. L. *Science* **1984**, *223* (4633), 283−285.
(5) Atalla, R. H.; Vanderhart, D. L. *Science* **1985**, *227* (4682), 79−79.
(6) Liu, H.; Hsieh, Y.-L. *J. Polym. Sci., Part B: Polym. Phys.* **2002**, *40* (18), 2119−2129.
(7) Kim, C.-W.; Kim, D.-S.; Kang, S.-Y.; Marquez, M.; Joo, Y. L. *Polymer* **2006**, *47*, 5097−5107.
(8) Battista, O. A. *Ind. Eng. Chem.* **1950**, *42*, 502−507.
(9) Battista, O. A. *Microcrystal Polymer Science*; McGraw-Hill Book Company: New York, 1975.
(10) Fleming, K.; Gray, D. G.; Matthews, S. *Chem−Eur. J.* **2001**, *7* (9), 1831−1835.
(11) Lima, M. M. D.; Borsali, R. *Macromol. Rapid Commun.* **2004**, *25* (7), 771−787.
(12) Araki, J.; Wada, M.; Kuga, S.; Okano, T. *Colloids Surf., A: Physicochem. Eng. Aspects* **1998**, *142* (1), 75−82.
(13) Orts, W.; Godbout, L.; Marchessault, R.; Revol, J.-F. *Macromolecules* **1998**, *31* (17), 5717−5725.
(14) Saito, T.; Nishiyama, Y.; Putaux, J. L.; Vignon, M.; Isogai, A. *Biomacromolecules* **2006**, *7* (6), 1687−1691.
(15) Turbak, A. F.; Snyder, F. W.; Sandberg, K. R. *J. Appl. Polym. Sci.: Appl. Polym. Symp.* **1983**, *37*, 815.
(16) Herrick, F. W.; Casebier, R. L.; Hamilton, J. K.; Sandberg, K. R. *J. Appl. Polym. Sci.: Appl. Polym. Symp.* **1983**, *37*, 797−813.
(17) Nakagaito, A. N.; Yano, H. *Appl. Phys. A: Mater. Sci. Process.* **2004**, *78* (4), 547−552.
(18) Berglund, L. A. Cellulose-based nanocomposites. In *Natural Fibers, Biopolymers, and Biocomposites*; Mohanty, A. K., Misra, M., Drzal, L. T., Eds.; CRC Press: 2005.
(19) Nakagaito, A. N.; Yano, H. *Appl. Phys. A: Mater. Sci. Process.* **2005**, *80* (1), 155−159.
(20) Nakagaito, A. N.; Iwamoto, S.; Yano, H. *Appl. Phys. A: Mater. Sci. Process.* **2005**, *80* (1), 93−97.
(21) Henriksson, M.; Henriksson, G.; Berglund, L. A.; Lindström, T. *Eur. Polym. J.* **2007**, in press.
(22) Ono, H.; Shimaya, Y.; Sato, K.; Hongo, T. *Polym. J.* **2004**, *36* (9), 684−694.
(23) Tatsumi, D.; Ishioka, S.; Matsumoto, T. *J. Soc. Rheol., Jpn.* **2002**, *30* (32), 27−32.
(24) Rudraraju, V. S.; Wyandt, C. M. *Int. J. Pharm.* **2005**, *292* (1−2), 53−61.
(25) Rudraraju, V. S.; Wyandt, C. M. *Int. J. Pharm.* **2005**, *292* (1−2), 63−73.
(26) Lowys, M.-P.; Desbrieres, J.; Rinaudo, M. *Food Hydrocolloids* **2001**, *15* (1), 25−32.
(27) Ono, H.; Yamada, H.; Matsuda, S.; Okajima, K.; Kawamoto, T.; Iijima, H. *Cellulose* **1998**, *5* (4), 231−247.
(28) Ono, H.; Shimaya, Y.; Hongo, T.; Yamane, C. *Trans. Mater. Res. Soc. Jpn.* **2001**, *26* (2), 569−572.
(29) Engström, A.-C.; Ek, M.; Henriksson, G. *Biomacromolecules* **2006**, *7*, 2027−2031.
(30) Hausalo, T.; Söderhjelm, L. Chemical Analysis of Pulps. In *Pulp and Paper Testing*; Levlin, J.-E.; Söderhjelm, L., Eds.; Fapet Oy: Jyväskylä, Finland, 1999; pp 39−63.
(31) Hiltunen, E. Papermaking Properties of Pulp. In *Pulp and Paper Testing*; Levlin, J.-E.; Söderhjelm, L., Eds.; Fapet Oy: Jyväskylä, Finland. 1999; pp 111−135.
(32) Larsson, P.; Wickholm, K.; Iversen, T. *Carbohydr. Res.* **1997**, *302*, 19−25.
(33) Wickholm, K.; Larsson, P.; Iversen, T. *Carbohydr. Res.* **1998**, *312*, 123−129.
(34) Press, W.; Flannery, S.; Vetterling, W. In *Numerical Recipes, The Art of Scientific Computing;* Cambridge University Press: Cambridge, U.K., 1988; Chapter 14.4.
(35) Katz, K.; Beatson, R. P.; Scallan, A. M. *Sven. Papperstid.* **1984**, *87* (6), R48.

(36) Ebeling, T.; Paillet, M.; Borsali, R.; Diat, O.; Dufresne, A.; Cavaille, J. Y.; Chanzy, H. *Langmuir* **1999**, *15* (19), 6123−6126.
(37) Bercea, M.; Navard, P. *Macromolecules* **2000**, *33* (16), 6011−6016.
(38) te Nijenhuis, K.; Mijs, W. J. *Chemical and Physical Networks Formation and Control of Properties*; John Wiley & Sons: Chichester, U.K., 1998; Vol. 1.
(39) Guenet, J.-M. *J. Rheol.* **2000**, *44* (4), 947−960.
(40) de Gennes, P.-G. *Scaling Concepts in Polymer Physics*; Cornell University Press: Ithaca, New York, 1979.
(41) Sahimi, M. *Phys. Rep.* **1998**, *306* (4-6), 213−395.
(42) Tamai, N.; Tatsumi, D.; Matsumoto, T. *Biomacromolecules* **2004**, *5* (2), 422−432.
(43) Doi, M.; Edwards, S. *Chem. Soc., Faraday Trans.* **1978**, *74*, 1818.
(44) Jones, J. L.; Marques, C. M. *J. Phys. Fr.* **1990**, *51*, 1113−1127.
(45) *Soft Matter Physics*; Daoud, M., Williams, C. E., Eds.; Springer-Verlag: Berlin, 1999.
(46) Onogi, S.; Asada, T. *Rheology*; Asarita, G., Marrucci, G., Nicolais, L., Eds.; Plenum: New York, 1980; Vol. 3, p 127.

BM061215P